

Comparing Exploration–Exploitation Strategies of LLMs and Humans: Insights from Standard Multi-armed Bandit Tasks

Ziyuan Zhang¹, Darcy Wang², Ningyuan Chen³, Rodrigo Mansur⁴, Vahid Sarhangian¹

¹Dept. of Mechanical & Industrial Engineering, University of Toronto

²Dept. of Computer Science, University of Toronto

³The Rotman School of Management, University of Toronto

⁴Dept. of Psychiatry, University of Toronto

{zyuan.zhang, darcy.wang}@mail.utoronto.ca, ningyuan.chen@utoronto.ca,
Rodrigo.Mansur@uhn.ca, sarhangian@mie.utoronto.ca

May 16, 2025

Abstract

Large language models (LLMs) are increasingly used to simulate or automate human behavior in complex sequential decision-making tasks. A natural question is then whether LLMs exhibit similar decision-making behavior to humans, and can achieve comparable (or superior) performance. In this work, we focus on the exploration-exploitation (E&E) tradeoff, a fundamental aspect of dynamic decision-making under uncertainty. We employ canonical multi-armed bandit (MAB) tasks introduced in the cognitive science and psychiatry literature to conduct a comparative study of the E&E strategies of LLMs, humans, and MAB algorithms. We use interpretable choice models to capture the E&E strategies of the agents and investigate how explicit reasoning, through both prompting strategies and reasoning-enhanced models, shapes LLM decision-making. We find that reasoning shifts LLMs toward more human-like behavior, characterized by a mix of *random* and *directed* exploration. In simple stationary tasks, reasoning-enabled LLMs exhibit similar levels of random and directed exploration compared to humans. However, in more complex, non-stationary environments, LLMs struggle to match human adaptability, particularly in effective directed exploration, despite achieving similar regret in certain scenarios. Our findings highlight both the promise and limits of LLMs as simulators of human behavior and tools for automated decision-making and point to potential areas of improvements.

1 Introduction

Large Language Models (LLMs), while originally developed for text generation, are increasingly used as simulators of human behavior. Researchers across disciplines have leveraged LLMs to simulate how humans respond to different stimuli, such as consumer choices and preference [1, 2, 3, 4], political messaging [5], moral context [6], and even interactive daily social routines [7]. Additionally, there

is growing interest to use LLMs to support or automate decision-making in complex sequential settings (e.g., [8, 9, 10]). Recent advances in explicit reasoning techniques through prompting (e.g., Chain-of-Thought [11, 12]), reinforcement learning, and tool-augmented reasoning (see [13] and [14] for recent surveys) have substantially improved LLM performance on multi-step reasoning tasks, thus potentially expanding their ability to simulate or automate dynamic decision-making tasks in real-world settings. However, it remains unclear whether LLMs can sufficiently capture the dynamic, adaptive, and cognitively grounded aspects of human decision-making, or achieve human-level (or better) performance. This motivates the central research question of our work: *Can LLMs reliably simulate human behavior and support automated decision making in sequential tasks under uncertainty?*

In this paper, we focus on a fundamental aspect of decision-making, namely the *exploration-exploitation* (E&E) tradeoff, arising whenever individuals must choose between leveraging known rewarding options (exploitation) and seeking out new possibilities that might lead to better outcomes (exploration). In cognitive science and psychiatry, patterns of E&E have been extensively studied to understand normative and impaired decision processes [15, 16], highlighting their central role in driving human behavior. A common experimental paradigm for studying this tradeoff is the (computerized) *multi-armed bandit (MAB) task*, in which participants repeatedly choose among several options with unknown reward distributions. Whereas the extensive literature in computer science, economics, operations research, and statistics focuses on the design and regret analysis for MAB algorithms (see, e.g., [17, 18]), the cognitive science literature employs MAB tasks to understand how humans navigate the E&E tradeoff. A key finding in this literature is that humans use a mixture of random and directed exploration. In *random exploration*, individuals sample options unpredictably, introducing stochasticity into choice behavior without explicit consideration of uncertainty. In contrast, *directed exploration* involves systematically selecting options associated with higher uncertainty in order to maximize information gain [19, 20]. These findings underscore that human exploration is not purely random, but often goal-directed and informed by subjective uncertainty estimates and internal models of the environment. Systematic deviations from this pattern have been observed in various psychiatric populations, such as reduced directed exploration in depression [21] and increased random exploration in attention-deficit/hyperactivity disorder (ADHD) [22] or schizophrenia [23].

We investigate how LLMs navigate the E&E tradeoff by adopting two widely-used MAB tasks from the cognitive science literature [16, 24]. We use standard interpretable choice models to characterize the underlying decision strategies of three commercial LLMs and compare them with those of human agents as well as MAB algorithms. We use the same tasks and with matched experimental conditions across the agents to facilitate comparison. Previous studies (e.g., [25, 26, 27]) have examined E&E trade-offs in LLMs, but using simple 2-armed tasks. A key aspect of our work is investigating how enhanced reasoning capabilities, achieved either via explicit prompting [28, 11, 12, 29] or reasoning-optimized model architectures (e.g., [30]), impact decision-making behavior of LLMs. Our main *contributions* and *findings* can be summarized as follows.

First, we conduct a comprehensive comparative study of the E&E strategies of commercial

LLMs, human participants, and MAB algorithmic using two standard MAB tasks: a stationary 2-armed task, and a more complex 4-armed non-stationary task. Although the behavior of LLMs and algorithmic baselines can be simulated, as done in earlier studies, a key contribution of our work is the use of two datasets collected from human participants performing the same MAB tasks under controlled experimental conditions. This enables more reliable and fair comparisons between human and artificial agents.

Second, we estimate and compare the behavior of the agents in terms of directed and random exploration, among other parameters. This allows us to investigate whether LLMs use a mixed exploration strategy as in humans and how reasoning capabilities impact E&E strategies. We find that LLMs exhibit different E&E strategies from humans and MAB algorithms, in terms of both the overall level and the types of exploration. Reasoning capabilities increase the direct exploration of LLMs in both tasks, and allow them to reach human levels for the stationary task. However, in the more complex non-stationary task, LLMs fail to engage in effective directed exploration compared to humans.

Third, we compare the agents in terms of model-free performance metrics of regret and exploitation rate over time. This allows us to investigate how the observed differences in the E&E strategies translate to performance gaps. We find that basic LLMs can achieve similar regret compared to humans in the stationary task. However, they exhibit more variable exploitation rates in the non-stationary task and accumulate regret much faster than humans. Explicit reasoning significantly improves the performance of LLMs, bringing their regrets to levels comparable to humans in certain scenarios.

2 Related Work

E&E Tradeoffs in Humans. Investigating the E&E strategies of humans and how they are impacted by various interventions or disorders has been an active area of research in the psychiatry literature [23], as well as in cognitive psychology [31] and neuroscience [15]. MAB tasks are a widely used experimental paradigm for studying the E&E behavior in humans. Variants include non-stationary 4-armed bandit tasks with decaying reward ([16, 32, 33, 34, 35, 23]), stationary two-armed bandit tasks [24], and horizon tasks comparing exploration under different information conditions [19, 20]. Computational models that integrate learning and choice rules are central to characterizing human E&E strategies. Learning rules, such as a Bayesian learner model [16] or temporal difference (TD) learning [36, 37, 35], estimate the expected outcomes for each option as the tasks evolve. Choice rules then map these estimates into decisions, typically employing softmax functions [16, 32] or probit regression [24]. In this work, we use these models to investigate the E&E strategies of LLMs and compare them with humans in the same tasks.

Understanding the decision-making behavior of LLMs. Several studies have investigated various aspects of decision-making behavior for LLMs, including risk preferences and loss aversion [38, 25], and trust behavior [39]. [25] studies several behavioral aspects of GPT3 using standard tasks

from cognitive psychology, including the Horizon task (a variant of the two-armed MAB task) to investigate E&E strategies. Our study expands that of [25] in several ways using the more complex 4-armed task with decaying rewards, and considering other agents. Consistent with their findings, we also find that LLMs engage in limited directed exploration and that LLMs can have low-regret in the stationary two-armed task. In contrast, we find that LLMs can have large regret in the more complex 4-armed task, but reasoning can significantly boost their exploration capabilities and lower regret. A related body of work focuses on understanding the role-behavior capabilities of LLMs (i.e., impersonating different human roles). [40, 41] examine the decision-making behavior of LLMs in-context, including their E&E strategies using two-armed MAB tasks.

LLMs for Optimal Dynamic Decision-Making. A growing body of literature investigates the performance of LLMs in dynamic (sequential) decision-making tasks (e.g., [8, 9, 42, 43, 44, 10, 45]). Because managing the E&E tradeoff is a key component of optimal dynamic decision-making, several studies have explored and aimed to improve LLMs’ capabilities in MAB tasks, in particular focusing on their ability to make optimal decisions through explorations [27, 26, 46]. In contrast, we focus on understanding the E&E strategies of LLMs in MAB tasks and, in particular, how they differ from those of human agents. We also show that reasoning capabilities could substantially improve the performance of LLMs in terms of regret.

LLMs for Simulating Human Behavior. There is also growing interest in using LLMs to simulate human behavior across diverse areas and disciplines, including economics and marketing [47, 3, 2, 4], cognitive science [6], computer science [1, 7], and political science [5]. Our comparative results provide insights into whether LLMs exhibit similar E&E strategies compared to humans, a key aspect of decision-making in many of the above application areas.

3 Experimental Setup

In this section, we describe the experimental setup used to evaluate and compare agents’ behavior. We detail the design of the two bandit tasks, the prompt design procedures for eliciting LLM decisions, and the human datasets and algorithmic benchmarks used in the experiments.

3.1 Multi-armed Bandit (MAB) Tasks

We begin by formally defining a geneal MAB task. There are $K \in \mathbb{N}$ available arms (actions). The decision-maker interacts with the system over T discrete time-steps, or *rounds*, indexed by $t \in [T] := \{1, \dots, T\}$. Each arm $k \in [K]$ has a possibly time-dependent reward distribution $P_k(t)$ that is independent of other arms. At each round t , the decision-maker selects an arm $a_t \in [K]$ according to some policy π and receives a reward $r_t \sim P_{a_t}(t)$. This generates a trajectory of actions and rewards $\{a_1, r_1, \dots, a_T, r_T\}$ for a single *trial* of the task. We consider two variants of MAB tasks from the literature which we briefly introduce next.

Stationary 2-armed bandit. The first task is originally proposed in [24] and subsequently used in several studies, e.g., [41, 20, 40]. Each agent completes 20 trials of a 2-armed bandit task with $T = 10$ rounds in each trial. Both arms generate stochastic (but stationary) rewards. At the start of each trial, the mean rewards for two arms, μ_1 and μ_2 , are independently sampled from a Gaussian distribution $\mathcal{N}(0, 100)$. In each round, the reward associated with arm $k \in \{1, 2\}$ is drawn from $\mathcal{N}(\mu_k, \sigma_0^2)$, with $\sigma_0^2 \equiv 10$ fixed across arms and rounds.

Non-stationary 4-armed bandit. The second task is originally proposed in [16] and has been widely adopted in the cognitive psychiatry literature, e.g., [32, 33, 34, 35]. To encourage agents' exploration behavior, this task introduces non-stationary mean rewards that follow a diffusion process. Each subject completes one trial of the task with $T = 300$ rounds [32], or two trials with $T = 150$ rounds [16]. The reward in round t of arm k is drawn from a Gaussian distribution with a time-varying mean $\mu_{k,t}$, and a fixed variance σ_0^2 , i.e., $r_{k,t} \sim \mathcal{N}(\mu_{k,t}, \sigma_0^2)$. The variance of the reward is set to $\sigma_0^2 = 4$. The mean reward for each arm follows a decaying Gaussian random walk given by $\mu_{k,t+1} = \lambda\mu_{k,t} + (1 - \lambda)\theta + \omega_t$, for $t \in \{1, \dots, T - 1\}$ with $\mu_{1,1} = 20, \mu_{2,1} = 40, \mu_{3,1} = 60, \mu_{4,1} = 80$. In the formula, λ and θ represent the decaying rate and long-term mean, respectively and are set to $\lambda = 0.9836$ and $\theta = 50$. Furthermore, ω_t denotes the diffusion noise and is drawn independently in each round from a zero-mean Gaussian distribution with variance $\sigma_d^2 = 2.8$. Different from the 2-armed tasks, three groups of reward sequences (for all arms) are *pre-generated* before the experiment. Each participant is then randomly assigned to one of the reward groups.

3.2 Agents Completing the MAB Tasks

In this section, we introduce the agents that have completed the tasks whose data have been recorded. They include three categories: human participants, LLM agents, and popular MAB algorithms.

Human participants. We use two datasets from previous studies collected from human participants. The first dataset [24] consists of 45 human participants completing the stationary 2-armed bandit task, and is collected via the Amazon Mechanical Turk (MTurk) platform¹. For each trial of each participant, the dataset includes the fixed mean rewards for both arms; for each round within a trial, it records the participant's selected arm and the corresponding integer reward observed by the participant. For the non-stationary 4-armed bandit task ($T = 300$), we use the dataset [48] from a controlled lab experiment², reported in [32]. The dataset consists of 31 participants, and each participant is randomly assigned to one of three pre-generated reward groups, with all reward sequences fixed in advance. For each round, the dataset records the participant's selected arm and the corresponding reward according to the assigned reward group.

In both MAB tasks, the participants are explicitly informed that their main objective is to maximize their total reward. Compensation consisted of a fixed payment for participation, with an additional performance-based bonus in the 4-armed bandit task. See Appendix A.1 for more details.

¹Publicly available at: <https://github.com/sjgershm/exploration>

²Dataset available at Zenodo upon request: <https://doi.org/10.5281/zenodo.3872973>

LLM agents. We employ LLMs as participants of the two MAB tasks described above. We closely follow the original experimental protocols for both tasks, ensuring that LLMs receive equivalent information throughout the task as the human participants. We test a set of popular commercial LLMs, namely GPT-4O-MINI, GEMINI-1.5-PRO, and DEEPSEEK-V3, along with reasoning models GPT-o3-MINI, GEMINI-1.5-FLASH, and DEEPSEEK-R1. Version numbers are omitted hereafter for simplicity.

To ask LLMs to complete both MAB tasks, we first provide with a system prompt describing the bandit task and outlining the main objective. Similar to human participants. LLMs are instructed to aim at maximizing their total reward. Then in each round, we send a prompt first summarizing the chosen arms and received rewards of past rounds in JSON format. We then instruct the LLMs to make their decisions, using two variations of prompts: standard and Chain-of-Thought (CoT). In the standard version, we ask them to directly make their choices without any explanation; in the CoT version, we encourage them to “*think out loud*” to facilitate reasoning. Examples of prompt designs are presented in Appendix A.3. Note that our CoT prompting is slightly different from formalized prompts such as “*Let’s think step by step.*” in the literature [11, 12]. This is because the MAB tasks do not involve well-defined and step-by-step mathematical reasoning. Nevertheless, this approach significantly elicits interpretable reasoning traces from LLMs (see Appendix A.3 for several illustrative examples). For each LLM model and prompting variation, we conduct 300 independent trials for the 2-armed bandit task and 15 for the 4-armed bandit task.

MAB algorithms. We include three popular MAB algorithms, the Upper Confidence Bound (UCB) algorithm [49, 50], Thompson Sampling (TS) [51], and ϵ -greedy [36]. See Appendix A.2 for the details in implementing these algorithms in our experiments. We refer to textbooks and surveys [17, 18] for a theoretical treatment of the algorithms such as their regret analyses and [52] for an empirical investigation. In particular, all three algorithms have been shown to learn the optimal arm and achieve near-optimal regret in stationary settings with proper hyperparameters, as the time horizon increases.

4 Choice Models and Estimation

In this section, we present the choice models used to characterize human and LLM decision-making. We describe two model classes based on softmax functions and probit regression, commonly used in the literature. We do not propose new models that may fit the data better, in order to compare to and benchmark against the observations made in prior studies. We then employ a hierarchical Bayesian approach for parameter estimation.

Choice models. For both model classes, we assume that agents form and update estimates of the expected value $Q_k(t)$ and standard deviation $S_k(t)$ of the mean payoff of each arm $k \in [K]$ and in each round t . These quantities are computed using an established Bayesian learner model [16] which is based on the Kalman filter [53, 54]; see Appendix B.1 for details.

The first class of choice models is based on the softmax function with increasing model complexity. Coefficient β is the *inverse temperature parameter*, which controls the degree of *random exploration*; ϕ represents the *uncertainty bonus*, capturing the extent of *directed exploration*; and ρ models *choice perseveration*, reflecting a subject's tendency to repeat previous choices:

$$P(a_t = k) = \frac{\exp\{\beta Q_k(t)\}}{\sum_{i=1}^K \exp\{\beta Q_i(t)\}}, \quad (\text{SM-1})$$

$$P(a_t = k) = \frac{\exp\{\beta[Q_k(t) + \varphi S_k(t)]\}}{\sum_{i=1}^K \exp\{\beta[Q_i(t) + \varphi S_i(t)]\}}, \quad (\text{SM-2})$$

$$P(a_t = k) = \frac{\exp\{\beta[Q_k(t) + \varphi S_k(t) + \rho \mathbb{I}_{(a_{t-1}=k)}]\}}{\sum_{i=1}^K \exp\{\beta[Q_i(t) + \varphi S_i(t) + \rho \mathbb{I}_{(a_{t-1}=i)}]\}}. \quad (\text{SM-3})$$

We adopt the following interpretation of these parameters from the literature [32]:

- Higher values of β lead to less random and exploratory choices and more “high-value” arms;
- Higher values of ϕ lead to more exploration of uncertain arms, similar to the principle of “optimism in the face of uncertainty” in the design of UCB-type algorithms;
- Higher values of ρ lead to more repeated choices of the same arm over consecutive periods.

The three softmax-based choice rules can be applied to both bandit tasks. Additionally, we consider a probit-regression-based choice rule specifically for the 2-armed bandit task [24], which incorporates the value difference $V_t = Q_1(t) - Q_2(t)$, the total uncertainty $TU_t = \sqrt{S_1^2(t) + S_2^2(t)}$, and the relative uncertainty $RU_t = S_1(t) - S_2(t)$ as covariates. In each round t , the choice probability is given by

$$P(a_t = 1) = \Phi \left(w_1 V_t + w_2 RU_t + w_3 \frac{V_t}{TU_t} \right), \quad (\text{Probit})$$

where $\Phi(\cdot)$ is the cumulative distribution function (CDF) of the standard Gaussian distribution with mean 0 and variance 1. The parameters have the following interpretation [55, 24]:

- Higher values of w_1 lead to more frequent choices of empirically higher-value arms, which captures the exploitative behavior of the agent;
- Higher values of w_2 lead to more frequent choices of arms with higher uncertainty, which is similar to ϕ in the softmax models;
- In addition to w_1 , w_3 is the *uncertainty normalized* value difference which characterizes the tendency to choose empirically high-value arms when the overall uncertainty is low. That is, for a fixed V_t , higher values of w_3 lead to more frequent choices of high-value arms when the trial is approaching the end and the agent has learned the mean reward of both arms quite accurately.

Parameter estimation. We use a hierarchical Bayesian approach [34, 32, 56, 57] to estimate parameters at the group level for each agent type, while also accounting for individual-level heterogeneity. In the context of behavioral modeling, this approach can yield more robust and interpretable estimates [56] compared to traditional maximum likelihood estimation (MLE), which has also been widely used in estimating choice parameters in the previous literature (e.g., [16, 35, 24]). Details of implementation and the hierarchical Bayesian structure could be found in Appendix B.2. We note that the hierarchical Bayesian approach estimates the population-level hyper-parameters, such as those controlling the distribution of β in (SM-1) among the participants, as well as the individual-level posterior distribution of the parameter for each agent. It thus allows for heterogeneity in the decision-making process across agents.

5 Experimental Results

In this section, we present the main empirical findings of our study. First, we compare the out-of-sample predictive performance of various choice models for the agents in both tasks. Next, we present and discuss the estimated parameters of the best-performing models. We refer to reasoning-optimized versions of each LLM with the suffix (R); e.g., DEEPSEEK (R) denotes DEEPSEEK-R1. This notation will be used consistently in all subsequent sections.

5.1 Out-of-Sample Performance of Different Choice Models

To conduct robust model selection based on out-of-sample predictive accuracy, we use a individual-level Bayesian leave-one-out (LOO) cross-validation (CV) approach [58]. For each subject, we compute the log-likelihood of their observed choices using model parameters estimated from the remaining subjects. To avoid the computational burden of refitting the model for each subject, we use Pareto-Smoothed Importance Sampling (PSIS) as an efficient approximation [58, 59]. Additional implementation details are provided in Appendix B.3.

Across both bandit tasks, the choice model with the highest score varied across LLMs. In the 2-armed bandit task, most LLMs achieve their best predictive performance under SM-2 and SM-3, while reasoning models and humans show strong compatibility with the Probit model (see Appendix C Table 1). In the 4-armed bandit task, SM-3 yields the best performance across all models, including for humans, suggesting that including the perseveration preference covariate is crucial for capturing the agents’ behavior. Accordingly, we select both the Probit and SM-3 models for the 2-armed bandit task, and the SM-3 model for the 4-armed bandit task. As shown in Table 1, these models consistently achieve the highest or near-highest normalized LOO-CV scores across agents. Even in cases where another model slightly outperforms them, their predictive performance remains highly competitive, making them well-suited for consistent cross-agent comparison.

5.2 Comparing Behavior Across Agents and Tasks

Model-based analysis of behavioral parameters. To understand how LLMs explore the arms differently from humans, we visualize the estimated parameters of the best-fitted choice model in each task. For each population-level mean parameter (μ_n^x in Figure 7 in Appendix B.2) we visualize the posterior mean and standard deviations using histograms. We compare these estimates to the corresponding posterior mean for human agents visualized using a dashed horizontal line. Detailed estimation results are presented in Tables 6-15 of Appendix C.

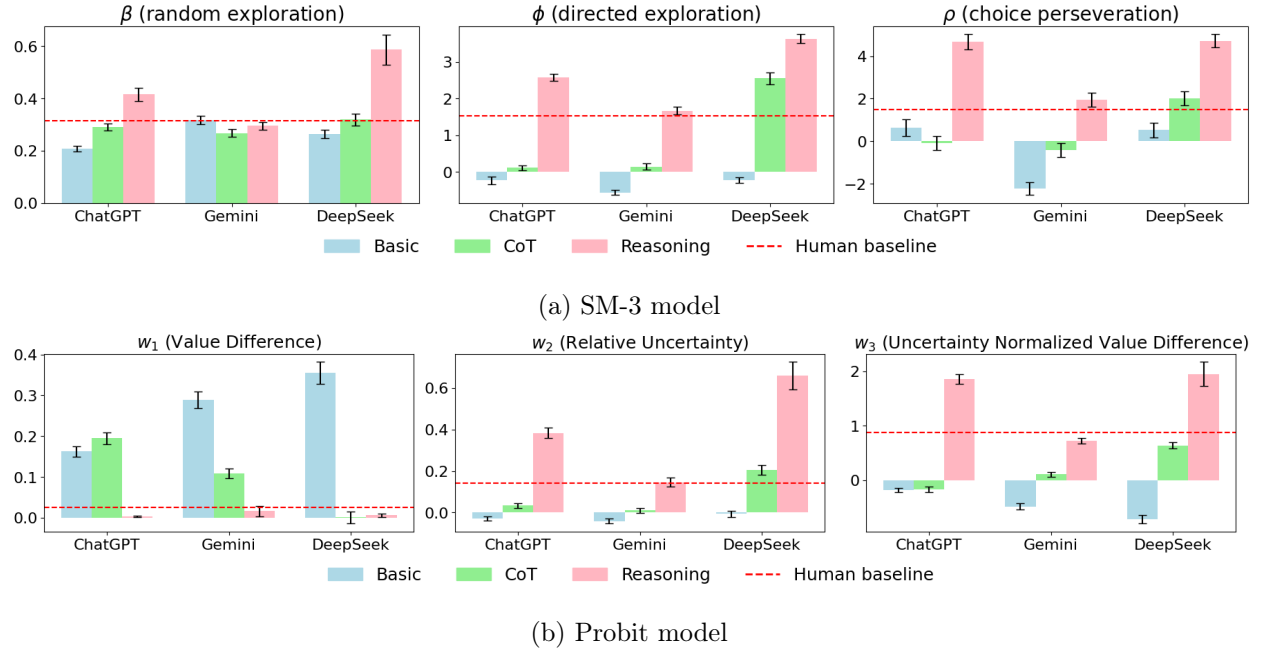


Figure 1: Visualizing the model parameters across agents in the 2-armed bandit task

Figure 1a and Figure 1b visualize the estimated parameters of the SM-3 and Probit model for the 2-armed task, respectively. We observe significant differences across LLMs and in contrast to humans. From the SM-3 model, we observe that basic LLMs engage in similar levels of random exploration (β), but do not exhibit directed exploration (ϕ) or choice preservation (ρ) at levels that human agents do. Enhancing their reasoning abilities consistently improves directed exploration and brings LLMs' behavior closer to human levels, particularly for GEMINI (R). For CHATGPT (R) and DEEPSEEK (R), we observe even higher parameter values than humans. A similar trend is observed for choice preservation.

From the Probit model, we observe that reasoning increases both w_2 and w_3 , indicating improved sensitivity to both forms of uncertainty, while we consistently observe that CHATGPT (R) and DEEPSEEK (R) exhibit higher levels than humans. Notably, w_3 reflects randomness adaptation to uncertainty—an effect not explicitly modeled in the softmax formulation. The increase in w_3 thus indicates more adaptive exploration, consistent with human-like behavior. Both humans and reasoning LLMs exhibit small weights on w_1 , but larger weights on w_3 , highlighting their reliance on total uncertainty rather than direct reward comparison.

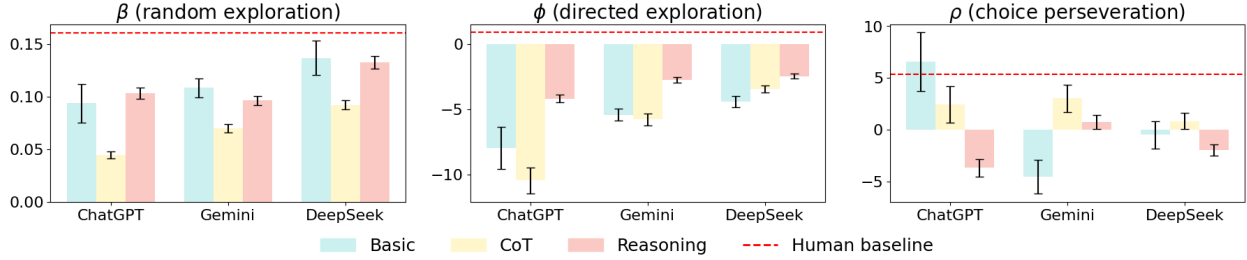


Figure 2: Visualizing the model parameters across agents in the 4-armed bandit task

Figure 2 visualizes the estimated parameters of the SM-3 model for the 4-armed task. Both basic and reasoning-enabled LLMs consistently exhibit higher levels of random exploration than humans. Although reasoning boosts sensitivity to uncertainty, as reflected by greater values of ϕ , the values remain negative across all LLM agents, suggesting that they fail to engage in effective directed exploration. Additionally, we do not observe a consistent pattern in choice perseveration by LLMs. In contrast, humans continue to engage in choice preservation.

Comparing the parameter estimates in the SM-3 model across the two MAB tasks, we observe that while reasoning shifts LLMs' exploration behavior toward the human baselines, the patterns differ by task. In the 2-armed task, reasoning improves alignment with human-like strategies, whereas in the more complex non-stationary 4-armed task, LLMs continue to exhibit lower levels of directed exploration and inconsistent choice preservation patterns.

In order to assess whether LLMs systematically follow algorithmic patterns, we also compare their parameter estimates to those derived from MAB algorithms. We find that LLMs do not systematically align with any single algorithmic strategy (see Appendix C, Tables 3 and 4 for detailed comparisons).

Model-free analysis of descriptive metrics. We next analyze agents' behavior using model-free metrics. Specifically, we focus on two key metrics of *exploitation rate* and *cumulative regret*.

The exploitation rate measures how often an agent selects the arm with the highest observed mean reward. Specifically, we define an action as *exploitative* if the agent chooses the option with the highest estimated mean among all arms at that round. In both bandit tasks, we calculate the average exploitation rate across all participants or replications for each agent type (e.g., humans, LLMs).

For both MAB tasks, we report the average exploitation rates across agents. In the 2-armed task, exploitation rates are consistently high across agents and closely match the levels achieved by algorithmic baselines (see Appendix C Table 2). In the 4-armed task with a longer horizon ($T = 300$), we track how agents' exploitation rates evolve by computing them across increasing time windows (e.g., $\tau = 10, 20, 30$ rounds, and so on). This helps reveal how different agents adapt their exploitation strategy. To reduce visual clutter, we include only UCB as the representative algorithmic baseline in the main figure.

As shown in Figure 3, LLMs exhibit highly dynamic exploitation behavior in the 4-armed bandit

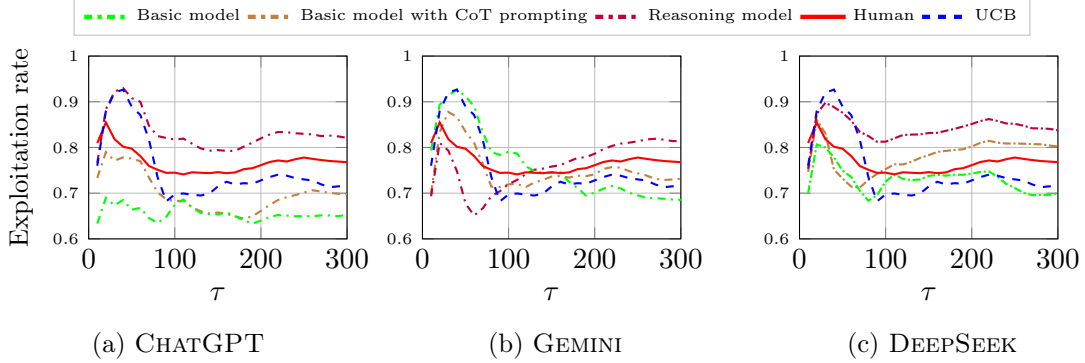


Figure 3: Exploitation rate over time in the 4-armed bandit task across agents

task. Unlike human agents, whose exploitation rate remains relatively stable over time, LLMs show large fluctuations and typically reach a peak around round 50. Interestingly, UCB displays a similar early peak, suggesting that both LLMs and UCB tend to over-commit to certain arms early on, assuming the rewards are fixed. They only begin to adjust after observing enough evidence that the rewards are changing. This highlights a gap in adaptive capabilities, with humans demonstrating more adaptive adjustments to evolving reward structures.

The second metric, cumulative regret, quantifies the performance gap between the agent’s choices and the optimal arm. In the 2-armed bandit task, the reward means μ_1 and μ_2 are themselves random variables drawn from a prior distribution at the beginning of each trial. This motivates the use of *Bayesian regret*, which averages the performance of a policy over the prior distribution of reward means. More precisely, we compute the regret for each agent type across N independent trials. In trial $n \in [N]$, a new pair of reward means $\mu_{n,1}, \mu_{n,2}$ is drawn. Suppose arm $a_{n,t}$ is selected in round $t \in [T]$. The *empirical Bayesian regret* up to round $\tau \in [T]$ is computed by averaging over all trials of a given agent type: $\widehat{\text{BayesRegret}}_{\text{agent}}(\tau) = \frac{1}{N} \sum_{n=1}^N \sum_{t=1}^{\tau} (\max\{\mu_{n,1}, \mu_{n,2}\} - \mu_{n,a_{n,t}})$.

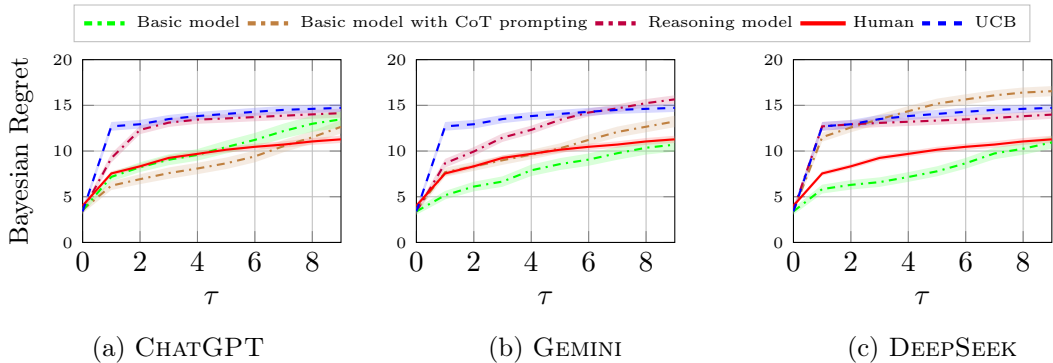


Figure 4: Empirical regret in the 2-armed bandit task across agents. Lines represent the average cumulative regret across trials within a given agent type; shaded areas denote ± 1 standard error.

For the 4-armed bandit task, recall that the reward sequences follow one of the three pre-defined sets (group 1, 2, and 3). For each agent type (humans, LLMs, algorithms), we average the

regret across all N trials. More precisely, let $G_n \in \{1, 2, 3\}$ denote the reward group assignment to trial $n \in [N]$, and $r_{g,k,t}$ denote the reward of arm $k \in [K]$ at round $t \in [T]$ ($K = 4, T = 300$) in group $g \in \{1, 2, 3\}$. Let $a_{n,t}$ be the action chosen in trial n at round t . The average *realized regret* for a given agent type up to round $\tau \in [T]$ is defined as: $\widehat{\text{RealizedRegret}}_{\text{agent}}(\tau) = \frac{1}{N} \sum_{n=1}^N \sum_{t=1}^{\tau} (\max_{k \in [K]} r_{G_n, k, t} - r_{G_n, a_{n,t}, t})$.

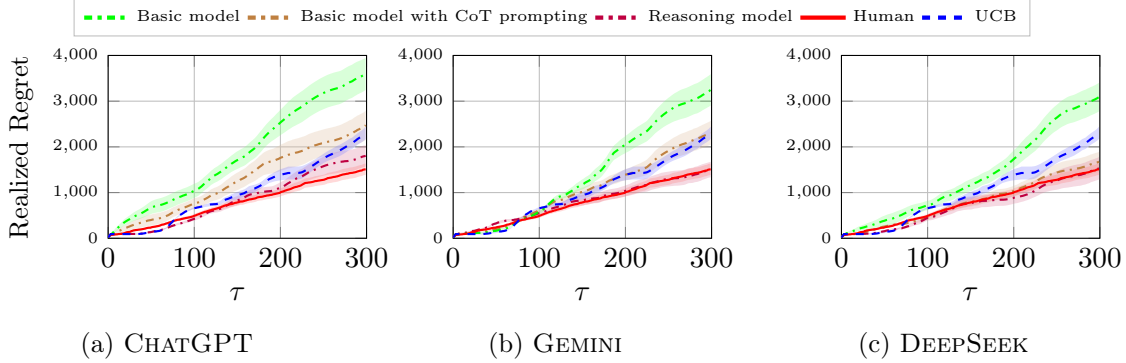


Figure 5: Empirical regret in the 4-armed bandit task across agents. Lines represent the average cumulative regret across trials within a given agent type; shaded areas denote ± 1 standard error.

Comparing the performance across agents and tasks, as shown in Figure 4, the cumulative regret remains low across all agents in the 2-armed task. The differences between agents' regrets are roughly equivalent to the regret incurred by a single suboptimal arm choice. While algorithms such as TS and ϵ -greedy are known to perform well in the long run, their short-run performance over just 10 rounds is slightly weaker than that of humans and LLMs (see Table 5 in Appendix C). In contrast, we observe that while human agents consistently achieve the lowest regret in the 4-armed bandit task, both LLMs and algorithms do much worse (see Figure 5). Enhancing LLMs with reasoning across three models substantially reduces their regret, bringing their performance closer to human level and surpassing standard algorithms, especially for GEMINI (R) and DEEPSEEK (R). These results suggest that explicit reasoning can significantly improve LLMs' E&E strategies, particularly in complex and non-stationary decision environments.

6 Key Observations and Implications

LLMs exhibit different E&E behavior compared to humans. The difference is reflected in terms of both the *overall level* of exploration and, more importantly, the *type* of exploration. Basic LLMs engage in more random exploration and less direct exploration (Figures 1 and 2). Moreover, their exploratory behavior varies drastically over time in the 4-armed bandit task (Figure 3). In particular, LLMs tend to explore more at the beginning and less toward the end of the horizon than humans. In contrast, human agents explore more; use both random and direct exploration strategies; explore at a more consistent level over time, and are more likely to repeat the previous choice.

Human agents achieve low regret. Human agents perform well in terms of regret in both tasks (Figures 4, 5), including in contrast to MAB algorithms that have been shown to have optimal asymptotic regret in stationary settings. We note that our experiments either have a short horizon (2-armed bandit) or are non-stationary (4-armed bandit), and hence do not satisfy the assumptions under which the performance guarantees are obtained. Nevertheless, our results reveal that human agents, just relying on their intuitions, can navigate decision-making in unknown and complex environments remarkably well.

Reasoning increases direct exploration and reduces regret for LLMs. Adding CoT to the prompts or using a reasoning LLM systematically changes the E&E behavior of LLMs. In particular, they increase the extent to which LLMs engage in direct exploration (Figures 1, 2). Interestingly, we observe that in the stationary task, LLMs with reasoning capability can behave similarly to humans, especially GEMINI (Figure 1). However, in the non-stationary task reasoning-enabled LLMs continue to exhibit higher levels of random exploration than humans. Moreover, the reasoning capability substantially improves the performance of LLMs measured in terms of regret.

Implications for using LLMs in dynamic decision-making tasks. First, our results highlight the limitations of LLMs in simulating the E&E behavior of humans, in particular in complex non-stationary settings: basic LLMs explore randomly and unevenly over time and lack humans' consistency, directed exploration, and repetition biases. Although augmenting LLMs with CoT or reasoning steers their behavior toward human-like E&E strategies, we continue to observe systematic deviations. The results suggest that embedding explicit prompts for uncertainty estimation and exploration reasoning could help align the behavior of LLMs with human strategies. Second, for automating decision-making, we find that basic LLMs achieve higher regret levels compared to humans in complex non-stationary tasks. Notably, this can be largely mitigated when reasoning and CoT-augmented LLMs are used. This suggests that targeted prompt design could elicit more effective exploration strategies and improve performance, even without modifying model architecture.

References

- [1] Gati V Aher, Rosa I Arriaga, and Adam Tauman Kalai. Using large language models to simulate multiple humans and replicate human subject studies. In *International Conference on Machine Learning*, pages 337–371. PMLR, 2023.
- [2] Neeraj Arora, Ishita Chakraborty, and Yohei Nishimura. AI–human hybrids for marketing research: Leveraging large language models (llms) as collaborators. *Journal of Marketing*, 89(2):43–70, 2025.
- [3] Ali Goli and Amandeep Singh. Frontiers: Can large language models capture human preferences? *Marketing Science*, 43(4):709–722, 2024.

- [4] James Brand, Ayelet Israeli, and Donald Ngwe. Using GPT for market research. *Harvard business school marketing unit working paper*, (23-062), 2023.
- [5] Lisa P Argyle, Ethan C Busby, Nancy Fulda, Joshua R Gubler, Christopher Rytting, and David Wingate. Out of one, many: Using language models to simulate human samples. *Political Analysis*, 31(3):337–351, 2023.
- [6] Danica Dillion, Niket Tandon, Yuling Gu, and Kurt Gray. Can AI language models replace human participants? *Trends in Cognitive Sciences*, 27(7):597–600, 2023.
- [7] Joon Sung Park, Joseph O’Brien, Carrie Jun Cai, Meredith Ringel Morris, Percy Liang, and Michael S Bernstein. Generative agents: Interactive simulacra of human behavior. In *Proceedings of the 36th annual ACM symposium on user interface software and technology*, pages 1–22, 2023.
- [8] Shibo Hao, Yi Gu, Haodi Ma, Joshua Jiahua Hong, Zhen Wang, Daisy Zhe Wang, and Zhiting Hu. Reasoning with language model is planning with world model. *arXiv preprint arXiv:2305.14992*, 2023.
- [9] Zhihan Liu, Hao Hu, Shenao Zhang, Hongyi Guo, Shuqi Ke, Boyi Liu, and Zhaoran Wang. Reason for future, act for now: A principled architecture for autonomous llm agents. In *Forty-first International Conference on Machine Learning*, 2024.
- [10] Xu Huang, Weiwen Liu, Xiaolong Chen, Xingmei Wang, Defu Lian, Yasheng Wang, Ruiming Tang, and Enhong Chen. Wese: Weak exploration to strong exploitation for llm agents. *arXiv preprint arXiv:2404.07456*, 2024.
- [11] Jason Wei, Xuezhi Wang, Dale Schuurmans, Maarten Bosma, Fei Xia, Ed Chi, Quoc V Le, Denny Zhou, et al. Chain-of-thought prompting elicits reasoning in large language models. *Advances in neural information processing systems*, 35:24824–24837, 2022.
- [12] Takeshi Kojima, Shixiang Shane Gu, Machel Reid, Yutaka Matsuo, and Yusuke Iwasawa. Large language models are zero-shot reasoners. *Advances in neural information processing systems*, 35:22199–22213, 2022.
- [13] Fengli Xu, Qianyue Hao, Zefang Zong, Jingwei Wang, Yunke Zhang, Jingyi Wang, Xiaochong Lan, Jiahui Gong, Tianjian Ouyang, Fanjin Meng, et al. Towards large reasoning models: A survey of reinforced reasoning with large language models. *arXiv preprint arXiv:2501.09686*, 2025.
- [14] Zixuan Ke, Fangkai Jiao, Yifei Ming, Xuan-Phi Nguyen, Austin Xu, Do Xuan Long, Minzhi Li, Chengwei Qin, Peifeng Wang, Silvio Savarese, et al. A survey of frontiers in LLM reasoning: Inference scaling, learning to reason, and agentic systems. *arXiv preprint arXiv:2504.09037*, 2025.

[15] Jonathan D Cohen, Samuel M McClure, and Angela J Yu. Should I stay or should I go? How the human brain manages the trade-off between exploitation and exploration. *Philosophical Transactions of the Royal Society B: Biological Sciences*, 362(1481):933–942, 2007.

[16] Nathaniel D Daw, John P O’doherty, Peter Dayan, Ben Seymour, and Raymond J Dolan. Cortical substrates for exploratory decisions in humans. *Nature*, 441(7095):876–879, 2006.

[17] Sébastien Bubeck, Nicolo Cesa-Bianchi, et al. Regret analysis of stochastic and nonstochastic multi-armed bandit problems. *Foundations and Trends® in Machine Learning*, 5(1):1–122, 2012.

[18] Tor Lattimore and Csaba Szepesvári. *Bandit algorithms*. Cambridge University Press, 2020.

[19] Robert C Wilson, Andra Geana, John M White, Elliot A Ludvig, and Jonathan D Cohen. Humans use directed and random exploration to solve the explore–exploit dilemma. *Journal of experimental psychology: General*, 143(6):2074, 2014.

[20] Robert C Wilson, Elizabeth Bonawitz, Vincent D Costa, and R Becket Ebitz. Balancing exploration and exploitation with information and randomization. *Current opinion in behavioral sciences*, 38:49–56, 2021.

[21] Ryan Smith, Samuel Taylor, Robert C Wilson, Anne E Chuning, Michelle R Persich, Siyu Wang, and William DS Killgore. Lower levels of directed exploration and reflective thinking are associated with greater anxiety and depression. *Frontiers in Psychiatry*, 12:782136, 2022.

[22] Merideth A Addicott, John M Pearson, Julia C Schechter, Jeffrey J Sapyta, Margaret D Weiss, and Scott H Kollins. Attention-deficit/hyperactivity disorder and the explore/exploit trade-off. *Neuropsychopharmacology*, 46(3):614–621, 2021.

[23] Flurin Cathomas, Federica Klaus, Karoline Guetter, Hui-Kuan Chung, Anjali Raja Beharelle, Tobias R Spiller, Rebecca Schlegel, Erich Seifritz, Matthias N Hartmann-Riemer, Philippe N Tobler, et al. Increased random exploration in schizophrenia is associated with inflammation. *npj Schizophrenia*, 7(1):6, 2021.

[24] Samuel J Gershman. Deconstructing the human algorithms for exploration. *Cognition*, 173: 34–42, 2018.

[25] Marcel Binz and Eric Schulz. Using cognitive psychology to understand GPT-3. *Proceedings of the National Academy of Sciences*, 120(6):e2218523120, 2023.

[26] Keegan Harris and Aleksandrs Slivkins. Should you use your large language model to explore or exploit? *arXiv preprint arXiv:2502.00225*, 2025.

[27] Akshay Krishnamurthy, Keegan Harris, Dylan J Foster, Cyril Zhang, and Aleksandrs Slivkins. Can large language models explore in-context? *arXiv preprint arXiv:2403.15371*, 2024.

[28] Shunyu Yao, Dian Yu, Jeffrey Zhao, Izhak Shafran, Tom Griffiths, Yuan Cao, and Karthik Narasimhan. Tree of thoughts: Deliberate problem solving with large language models. *Advances in neural information processing systems*, 36:11809–11822, 2023.

[29] Zhuosheng Zhang, Aston Zhang, Mu Li, and Alex Smola. Automatic chain of thought prompting in large language models. *arXiv preprint arXiv:2210.03493*, 2022.

[30] Daya Guo, Dejian Yang, Haowei Zhang, Junxiao Song, Ruoyu Zhang, Runxin Xu, Qihao Zhu, Shirong Ma, Peiyi Wang, Xiao Bi, et al. Deepseek-R1: Incentivizing reasoning capability in llms via reinforcement learning. *arXiv preprint arXiv:2501.12948*, 2025.

[31] Eric Schulz, Nicholas T Franklin, and Samuel J Gershman. Finding structure in multi-armed bandits. *Cognitive psychology*, 119:101261, 2020.

[32] Karima Chakroun, David Mathar, Antonius Wiesler, Florian Ganzer, and Jan Peters. Dopaminergic modulation of the exploration/exploitation trade-off in human decision-making. *Elife*, 9: e51260, 2020.

[33] Marieke Jepma, Erik T Te Beek, Eric-Jan Wagenmakers, Joop MA van Gerven, and Sander Nieuwenhuis. The role of the noradrenergic system in the exploration–exploitation trade-off: a psychopharmacological study. *Frontiers in human neuroscience*, 4:170, 2010.

[34] Anjali Raja Beharelle, Rafael Polanía, Todd A Hare, and Christian C Ruff. Transcranial stimulation over frontopolar cortex elucidates the choice attributes and neural mechanisms used to resolve exploration–exploitation trade-offs. *Journal of Neuroscience*, 35(43):14544–14556, 2015.

[35] Aaron M Bornstein, Mel W Khaw, Daphna Shohamy, and Nathaniel D Daw. Reminders of past choices bias decisions for reward in humans. *Nature Communications*, 8(1):15958, 2017.

[36] Richard S Sutton, Andrew G Barto, et al. *Reinforcement learning: An introduction*, volume 1. MIT press Cambridge, 1998.

[37] Leslie Pack Kaelbling, Michael L Littman, and Andrew W Moore. Reinforcement learning: A survey. *Journal of artificial intelligence research*, 4:237–285, 1996.

[38] Jingru Jia, Zehua Yuan, Junhao Pan, Paul E McNamara, and Deming Chen. Decision-making behavior evaluation framework for llms under uncertain context. *arXiv preprint arXiv:2406.05972*, 2024.

[39] Chengxing Xie, Canyu Chen, Feiran Jia, Ziyu Ye, Shiyang Lai, Kai Shu, Jindong Gu, Adel Bibi, Ziniu Hu, David Jurgens, et al. Can large language model agents simulate human trust behavior? In *The Thirty-eighth Annual Conference on Neural Information Processing Systems*, 2024.

[40] Leonard Salewski, Stephan Alaniz, Isabel Rio-Torto, Eric Schulz, and Zeynep Akata. In-context impersonation reveals large language models’ strengths and biases. *Advances in neural information processing systems*, 36:72044–72057, 2023.

[41] Chenglei Shen, Guofu Xie, Xiao Zhang, and Jun Xu. On the decision-making abilities in role-playing using large language models. *arXiv preprint arXiv:2402.18807*, 2024.

[42] Wenlong Huang, Fei Xia, Ted Xiao, Harris Chan, Jacky Liang, Pete Florence, Andy Zeng, Jonathan Tompson, Igor Mordatch, Yevgen Chebotar, et al. Inner monologue: Embodied reasoning through planning with language models. *arXiv preprint arXiv:2207.05608*, 2022.

[43] Sharath Chandra Raparthy, Eric Hambro, Robert Kirk, Mikael Henaff, and Roberta Raileanu. Generalization to new sequential decision making tasks with in-context learning. *arXiv preprint arXiv:2312.03801*, 2023.

[44] Shuang Li, Xavier Puig, Chris Paxton, Yilun Du, Clinton Wang, Linxi Fan, Tao Chen, De-An Huang, Ekin Akyürek, Anima Anandkumar, et al. Pre-trained language models for interactive decision-making. *Advances in Neural Information Processing Systems*, 35:31199–31212, 2022.

[45] Chanwoo Park, Xiangyu Liu, Asuman Ozdaglar, and Kaiqing Zhang. Do LLM agents have regret? a case study in online learning and games. *arXiv preprint arXiv:2403.16843*, 2024.

[46] Allen Nie, Yi Su, Bo Chang, Jonathan N Lee, Ed H Chi, Quoc V Le, and Minmin Chen. Evolve: Evaluating and optimizing llms for exploration. *arXiv preprint arXiv:2410.06238*, 2024.

[47] John J Horton. Large language models as simulated economic agents: What can we learn from homo silicus? Technical report, National Bureau of Economic Research, 2023.

[48] K. Chakroun, D. Mathar, A. Wiehler, F. Ganzer, and J. Peters. Dopaminergic modulation of the exploration/exploitation trade-off in human decision-making. Dataset, 2020. URL <https://doi.org/10.5281/zenodo.3872973>.

[49] Tze Leung Lai and Herbert Robbins. Asymptotically efficient adaptive allocation rules. *Advances in applied mathematics*, 6(1):4–22, 1985.

[50] Peter Auer, Nicolo Cesa-Bianchi, and Paul Fischer. Finite-time analysis of the multiarmed bandit problem. *Machine learning*, 47:235–256, 2002.

[51] William R Thompson. On the likelihood that one unknown probability exceeds another in view of the evidence of two samples. *Biometrika*, 25(3/4):285–294, 1933.

[52] Joannes Vermorel and Mehryar Mohri. Multi-armed bandit algorithms and empirical evaluation. In *European conference on machine learning*, pages 437–448. Springer, 2005.

[53] Brian DO Anderson and John B Moore. *Optimal filtering*. Courier Corporation, 2005.

[54] Rudolph Emil Kalman. A new approach to linear filtering and prediction problems. 1960.

- [55] Samuel J Gershman and Bastian Greshake Tzovaras. Dopaminergic genes are associated with both directed and random exploration. *Neuropsychologia*, 120:97–104, 2018.
- [56] Woo-Young Ahn, Nathaniel Haines, and Lei Zhang. Revealing neurocomputational mechanisms of reinforcement learning and decision-making with the hBayesDM package. *Computational Psychiatry*, 1:24–57, 2017. URL [doi:10.1162/CPSY_a_00002](https://doi.org/10.1162/CPSY_a_00002).
- [57] Woo-Young Ahn, Adam Krawitz, Woojae Kim, Jerome R Busemeyer, and Joshua W Brown. A model-based fmri analysis with hierarchical bayesian parameter estimation. 2013.
- [58] Aki Vehtari, Andrew Gelman, and Jonah Gabry. Practical bayesian model evaluation using leave-one-out cross-validation and waic. *Statistics and computing*, 27:1413–1432, 2017.
- [59] Aki Vehtari, Daniel Simpson, Andrew Gelman, Yuling Yao, and Jonah Gabry. Pareto smoothed importance sampling. *Journal of Machine Learning Research*, 25(72):1–58, 2024.
- [60] Bob Carpenter, Andrew Gelman, Matthew D Hoffman, Daniel Lee, Ben Goodrich, Michael Betancourt, Marcus Brubaker, Jiqiang Guo, Peter Li, and Allen Riddell. Stan: A probabilistic programming language. *Journal of statistical software*, 76:1–32, 2017.

A Experimental Setup Details

A.1 Human Data

In this section, we summarize the instructions provided to human participants in both bandit tasks. These instructions are adapted directly from the original studies [24, 32, 16] and used to form the prompts given to LLMs. Our goal is to ensure that human and LLM agents are presented with comparable information, such as task structure and task objectives, therefore enabling a fair comparison of their decision-making behavior.

2-armed bandit task. As reported in [24], each of the 45 participants play 20 independent games with each game consisting of 10 rounds and a distinct pair of slot machines. In each round, participants choose between two colored buttons representing slot machines and receive feedback in the form of integer rewards. The instructions also emphasized that the rewards are stochastic, and participants will win or lose points based on their choice. Each participant is paid a fixed amount \$1.5.

4-armed bandit task. Data corresponds to a double-blind, counterbalanced, placebo-controlled within-subjects study [32]. Participants perform a restless four-armed bandit task under three drug conditions including placebo. In our analysis, we exclusively use data obtained under the placebo, corresponding to 31 male participants who were mainly university students. All participants underwent a medical screening prior to the experiment, which included an electrocardiogram (ECG) and a health interview.

Each participant completes 300 rounds of a decision-making task involving four options, grouped into four blocks of 75 rounds. At each round, participants select one of four colored squares displayed on a screen, each representing a different ‘*bandit*’. After making a choice, they receive feedback indicating the number of points earned at that round.

Participants are informed that the goal is to maximize their total number of points throughout the task. The reward associated with each bandit drifts stochastically over time, following an independent Gaussian random walk. Importantly, participants are told that the payout would be tied to their total accumulated points, with 5 cents paid out for every 100 points earned. Specifically, they receive a fixed compensation of €270 and an additional performance-based bonus (€30–50). The full distribution of reward drift is not revealed, so participants must continuously track value estimates and adjust their exploration and exploitation strategies accordingly.

A.2 Algorithmic Baseline Setup

We implemented three standard algorithmic baselines for the MAB tasks: Upper Confidence Bound (UCB), Thompson Sampling (TS), and ϵ -greedy. These algorithms serve as interpretable performance benchmarks for comparison with human and LLM agents.

Upper Confidence Bound (UCB) In the K -armed bandit task, we first choose each arm once, and subsequently choose arm a_t on each round $t \in [T]$ according to:

$$a_t = \arg \max_{k \in [K]} \left(\hat{\mu}_t(k) + \hat{\sigma}_t(k) \cdot \sqrt{\frac{2 \log f(t)}{N_t(k)}} \right), \quad (1)$$

where,

- $f(t) = 1 + t \log^2(t)$;
- $\hat{\mu}_t(k), \hat{\sigma}_t(k)$ are the sample mean and sample standard deviation of rewards for arm k up to round t , respectively;
- $N_t(k)$ is the number of times arm k has been selected up to round t .

For initialization, when an arm has fewer than two samples, we set its sample deviation to a fixed prior value. Specifically, we set $\hat{\sigma}_t(k) = \sqrt{10}$ for the 2-armed bandit task and $\hat{\sigma}_t(k) = 2$ for the 4-armed bandit task for every arm $k \in [K]$.

This formulation adapts the classic asymptotically optimal UCB algorithm described in [18] by scaling the exploration term with the empirical standard deviation, thereby allowing the confidence interval to adjust based on the observed variability of each arm.

Thompson Sampling (TS). We adopt a Bayesian formulation with a Normal-Inverse-Gamma conjugate prior to model rewards with unknown variance. Assume rewards for each arm k are normally distributed:

$$r_t(k) \sim \mathcal{N}(\mu_k, \sigma_k^2) \quad (2)$$

The prior over (μ_k, σ_k^2) is given by:

$$\mu_k \mid \sigma_k^2 \sim \mathcal{N}(\mu_0, \sigma_k^2 / \lambda_0), \quad \sigma_k^2 \sim \text{Inv-Gamma}(\alpha_0, \beta_0) \quad (3)$$

At each round t , the algorithm samples from the posterior distribution of each arm and selects the arm with the highest sampled mean:

1. For each arm $k \in [K]$, sample:

$$\sigma_k^2 \sim \text{Inv-Gamma}(\alpha_k, \beta_k), \quad \tilde{\mu}_k \sim \mathcal{N}(\mu_k, \sigma_k^2 / \lambda_k)$$

2. Select arm:

$$a_t = \arg \max_{k \in [K]} \tilde{\mu}_k$$

3. Observe reward r_t , and update posterior for arm a_t as follows: Let the current parameters for the selected arm be $(\mu_{a_t}, \lambda_{a_t}, \alpha_{a_t}, \beta_{a_t})$. The posterior update is:

$$\begin{aligned}\lambda_{a_t} &\leftarrow \lambda_{a_t} + 1 \\ \mu_{a_t} &\leftarrow \frac{\lambda_{a_t} \mu_{a_t} + r_t}{\lambda_{a_t} + 1} \\ \alpha_{a_t} &\leftarrow \alpha_{a_t} + \frac{1}{2} \\ \beta_{a_t} &\leftarrow \beta_{a_t} + \frac{(r_t - \mu_{a_t})^2 \cdot \lambda_{a_t}}{2(\lambda_{a_t} + 1)}\end{aligned}$$

We use weakly informative priors in the 2-armed bandit task: $\mu_0 = 0$, $\lambda_0 = 1$, $\alpha_0 = 1$, $\beta_0 = 1$. And specifically, for the 4-armed bandit task, we set $\mu_0 = 50$, and other hyperparameters remain the same as in the 2-armed task.

ϵ -greedy For the ϵ -greedy algorithm, the agent selects the arm with the highest empirical mean with probability $1 - \epsilon$, and explores a random arm with probability ϵ :

$$a_t = \begin{cases} \arg \max_{k \in [K]} \hat{\mu}_t(k), & \text{with probability } 1 - \epsilon \\ \text{random arm,} & \text{with probability } \epsilon \end{cases} \quad (4)$$

We perform a grid search over $\epsilon \in \{0.1, 0.2, \dots, 0.9\}$ and find that $\epsilon = 0.1$ yields the lowest average regret across trials, so we adopt this value in all reported results.

To ensure that all algorithms start with well-defined estimates and avoid degenerate behavior in early rounds, we initialize each agent by pulling every arm once before applying the main decision rule. This warm-up phase ensures that all arms have at least one reward observation, which is particularly important for algorithms such as UCB (to avoid division by zero) and ϵ -greedy (to compute initial sample means). Although Thompson Sampling with a prior does not strictly require warm-up, we adopt the same initialization procedure for consistency across all baselines.

A.3 Prompt Design

Prompt: 2-armed Bandit Task

System: You are a real human agent playing with two slot machines, labelled 1 and 2, which provide uncertain rewards over time. You will play 20 games, each with a different pair of slot machines. Each game consists of 10 rounds. In each round, you are asked to choose one machine to play, and you will win or lose points based on your choice. Your objective is to maximize your total reward.

User:

If round == 1:

You are now performing game: {block_index}, round 1.

Else:

You are now performing game: {block_index}, round: {round_index}. Your history is provided below, which includes the “choice” you made and the corresponding “reward” you received in each round. Negative reward means losing points, and positive means winning points. {JSON}

Final instruction:

- V1: Which machine do you choose between machines 1 and 2? You can think out loud and answer the number.
- V2: Which machine do you choose between machines 1 and 2? Do not explain, answer the number.

Prompt: 4-armed Bandit Task

System: You are a real human agent playing with four slot machines, labelled 0, 1, 2, and 3, which provide uncertain rewards over time. You will play a single game consisting of 300 rounds. In each round, you choose one machine to play and receive points based on your choice. Your objective is to maximize your total reward throughout the experiment.

User:

If round == 1:

You are now performing round 1.

Else:

You are now performing round: {round_index}. Your history is provided below, which contains the “choice” you made and the corresponding “reward” you received in each “round.” {JSON}

Final instruction:

- V1: Which machine do you choose between machines 0, 1, 2 and 3? You can think out loud and answer the number.
- V2: Which machine do you choose between machines 0, 1, 2 and 3? Do not explain, answer the number.

An example of JSON format. Figure 6 shows an example of the JSON-formatted prompt shown to the LLM, which includes the choice and reward history from previous rounds:

```
[  
  {  
    "round": 1,  
    "choice": 2,  
    "reward": 45  
  },  
  {  
    "round": 2,  
    "choice": 1,  
    "reward": 21  
  }  
]
```

Figure 6: Example JSON-format prompt

Examples of LLMs’ responses To verify that our *“Think out loud”* prompt encourages LLMs to elicit a reasoning process similar to CoT prompting, we provide several illustrative examples of LLMs’ responses.

2-armed bandit task response: CHATGPT

Based on the history provided:

- In round 1, I chose machine 1 and received a reward of 21.
- In round 2, I chose machine 2 and received a reward of 6.
- In round 3, I chose machine 1 again and received a reward of 24.

So far, I have played machine 1 twice with good rewards (21 and 24 points) and machine 2 once with a lower reward (6 points). This suggests that machine 1 has been performing better for me based on the previous rounds.

I have a strong inclination to choose machine 1 again for this round, as it seems to have a higher average reward based on the history so far.

Therefore, I will choose: Arm 1

2-armed bandit task response: GEMINI

Machine 1 has yielded -8 and -6, for an average of -7.

Machine 2 has yielded -8, 0, and -9, for an average of -5.67.

While Machine 2's average is slightly better, the small sample size makes it hard to be confident.

Machine 2 also has shown more variability, having given a reward of 0 once. Since I've played machine 1 less, I'll try it again to get a better sense of its average reward.

2-armed bandit task response: DEEPSEEK

Let me analyze the history:

- Machine 1 was chosen twice, yielding rewards of 5 and 12. The average reward for Machine 1 is $(5 + 12) / 2 = 8.5$.
- Machine 2 was chosen once, yielding a reward of 10. The average reward for Machine 2 is 10.

Based on the average rewards, Machine 2 has a higher average reward (10) compared to Machine 1 (8.5). Therefore, I will choose Machine 2 to maximize my expected reward.

B Modeling and Estimation

In this section, we provide details on the Bayesian learner model, the hierarchical Bayesian structure for parameter estimation, and the cross-validation approach for model selection.

B.1 Bayesian Learning Model

Following [16], we adopt the Kalman Filter [53, 54] to estimate the expected value $Q_k(t)$ and uncertainty (standard deviation) $S_k(t)$ as described in Section 4 in the main paper. Assume the subject's belief over the true mean payoff $\mu_{k,t}$ for each arm $k \in [K]$ in round t follows a prior distribution $N(Q_k(t), S_k^2(t))$. If bandit a_t is chosen with payoff r_t , the posterior mean ($Q_{a_t}^{pos}(t)$) and variance ($S_{a_t}^{2pos}(t)$) are updated as,

$$Q_{a_t}^{pos}(t) = Q_{a_t}(t) + \kappa(t)(r_t - Q_{a_t}(t)), \quad (5)$$

$$S_{a_t}^{2pos}(t) = (1 - \kappa(t))S_{a_t}^2(t), \quad (6)$$

where $\kappa(t)$ is the Kalman gain for each trial t computed as

$$\kappa(t) = S_{a_t}^2(t) / (S_{a_t}^2(t) + \hat{\sigma}_0^2). \quad (7)$$

We set $Q_i(1) = Q(1)$, $S_i(1) = S(1)$ for each arm i at the beginning of each trial, implying that the subjects have the same estimates over different arms. Further, for arms that are not chosen in a

round, posteriors are equal to the prior in that round, i.e., $Q_i^{pos}(t) = Q_i(t), S_i^{pos}(t) = S_i(t), \forall i \neq c_t$. The priors of all bandits are updated between rounds according to,

$$Q_i(t+1) = \hat{\lambda}Q_i^{pos}(t) + (1 - \hat{\lambda})\hat{\theta}, \quad (8)$$

$$S_i(t+1) = \hat{\lambda}^2 S_i^{pos}(t) + \hat{\sigma}_d^2, \quad (9)$$

where $\hat{\sigma}_0^2, \hat{\sigma}_d^2, \hat{\theta}, \hat{\lambda}$ denote the subjects' estimates of the parameters in the diffusion process. Notice that in the stochastic 2-armed bandit task, since the mean reward for each arm remains constant, we have $\hat{\sigma}_d = \hat{\theta} = 0, \hat{\lambda} = 1$

B.2 Parameters Estimation & Hierarchical Bayesian Structure

Following [32, 24], in the 4-armed bandit task, we fix $\hat{\sigma}_0^2 = 4, \hat{\sigma}_d^2 = 2.8, \hat{\lambda} = 0.9836, \hat{\theta} = 50$ to be the same values as the true parameters in the diffusion process. We set $Q(1) = 50$ at the start of each independent trial. Similarly, in the 2-armed bandit task, we set $\hat{\sigma}_0^2 = 10$, and $Q(1) = 0, S(1) = 10$. These settings enable direct comparison with previous studies.

As shown in Figure 7, the model adopts a hierarchical structure in which any model parameter can be expressed in the form $x_{n,s}$. In other words, each parameter—whether it is β, ϕ, ρ in SM-based choice models or w_1, w_2, w_3 in the Probit regression model—is modeled in this generic form. Specifically, for each subject s in group n , the individual-level parameter $x_{n,s}$ is assumed to be drawn from a population-level normal prior distribution:

$$x_{n,s} \sim N(\mu_n^x, (\sigma_n^x)^2). \quad (10)$$

Here, each group corresponds to a specific category of agents (e.g., humans or LLMs), with each subject representing an individual human or a replication in an LLM experiment. The population-level mean μ_n^x is assigned a non-informative uniform prior over the interval $[x_{\min}, x_{\max}]$, while the population-level standard deviation σ_n^x is given a half-Cauchy prior, i.e.

$$\mu_n^x \sim \text{Uniform}(x_{\min}, x_{\max}), \quad \sigma_n^x \sim \text{half-Cauchy}(0, 1). \quad (11)$$

Specifically, in the softmax model, we set $\beta_{\min} = 0, \beta_{\max} = 10$, and $\phi_{\min} = \rho_{\min} = -\infty, \phi_{\max} = \rho_{\max} = \infty$, which corresponds to assigning non-informative priors on ϕ and ρ . And in the probit model, we set $w_{1\min} = 0, w_{2\min} = w_{3\min} = -1$ and $w_{1\max} = w_{2\max} = w_{3\max} = 5$.

We aim to infer the posterior distribution over all model parameters given the observed choice data. We then use Markov Chain Monte Carlo (MCMC) sampling to approximate the posterior. We implement this procedure using PyStan package, which interfaces with the Stan probabilistic

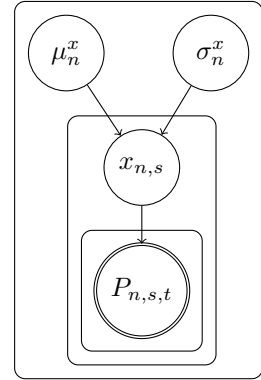


Figure 7: Hierarchical Bayesian Structure

programming framework [60]. Each model is fitted using four independent chains, each with 1000 iterations and 500 warm-up steps. Posterior summaries are computed from the combined post-warm-up samples.

B.3 Bayesian leave-one-out (LOO) cross-validation (CV)

We implement a individual-level Bayesian leave-one-out (LOO) cross-validation procedure to evaluate the out-of-sample predictive performance of each choice model. Specifically, we iteratively exclude one subject as the validation set, fit the model to the remaining subjects using MCMC sampling, and compute the predictive log-likelihood of the held-out subject’s choices. The resulting log-likelihood serves as the individual-level LOO-CV score, with higher scores indicating better predictive accuracy.

As full MCMC refitting for each held-out subject is computationally intensive, we adopt Pareto-Smoothed Importance Sampling (PSIS) [59] as an efficient approximation to exact LOO-CV. For each participant, we compute the sum of pointwise log-likelihoods across all rounds and trials based on posterior samples, and apply importance sampling to these individual-level likelihoods to estimate the leave-one-out predictive density. We implement this procedure using the `loo` function in the ArviZ package, applied to posterior draws generated from PyStan.

We conduct Section A and B on Google Colab with official LLM APIs.

C Experimental Results

We first present the key experimental results supporting our main analysis. Tables 1, 2, 3, 4 and 5 correspond to key findings referenced in the main text.

Table 1 presents individual-level LOO-CV results for both bandit tasks, comparing the predictive performance of different choice models across various LLMs and human data. Since the datasets vary in size, we normalize the LOO-CV scores the number of data points, allowing comparison across conditions.

Table 2 presents the average exploitation rates across independent trials for each agent type in the 2-armed bandit task. Panel 2a compares different LLMs, while Panel 2b reports the average rates for human participants and algorithmic baselines. We observe that exploitation rates are consistently high across agents and closely match the levels achieved by algorithmic baselines.

Table 3 reports the posterior means and standard deviations for estimated population-level mean parameters of SM-3 model and Probit model for MAB algorithms in the 2-armed bandit task.

Table 4 reports the posterior means and standard deviations for estimated population-level mean parameters of SM-3 model for MAB algorithms in the 4-armed bandit task.

As shown in Tables 3 and 4, benchmark algorithms exhibit distinct parameter patterns that are consistent with their underlying decision rules: In the 2-armed bandit task, UCB drives directed exploration through an uncertainty bonus (higher ϕ , w_2 and w_3), while TS and ϵ -greedy introduce greater random exploration (lower β) via prior sampling and stochastic choice mechanisms, respectively. In contrast, reasoning-enhanced LLMs display a mixed strategy, combining elements of both

Table 1: Normalized Individual-level LOO-CV score comparison. The best model is highlighted in boldface.

(a) 2-armed bandit					(b) 4-armed bandit		
Agent / Prompt	SM-1	SM-2	SM-3	Probit	SM-1	SM-2	SM-3
CHATGPT	-0.385	-0.381	-0.381	-0.382	-1.029	-0.059	-0.058
CHATGPT + CoT	-0.332	-0.331	-0.332	-0.337	-0.857	-0.319	-0.318
CHATGPT (R)	-0.357	-0.287	-0.229	-0.178	-0.567	-0.257	-0.255
GEMINI	-0.318	-0.312	-0.303	-0.302	-0.913	-0.104	-0.104
GEMINI + CoT	-0.364	-0.363	-0.363	-0.374	-0.764	-0.286	-0.286
GEMINI (R)	-0.395	-0.342	-0.334	-0.311	-0.570	-0.452	-0.452
DEEPEEK	-0.322	-0.319	-0.319	-0.332	-0.872	-0.103	-0.103
DEEPEEK + CoT	-0.413	-0.334	-0.324	-0.314	-0.581	-0.391	-0.391
DEEPEEK (R)	-0.360	-0.267	-0.195	-0.168	-0.484	-0.313	-0.312
Human Agents	-0.393	-0.346	-0.335	-0.329	-0.649	-0.633	-0.614
UCB	-0.116	-0.115	-0.114	-0.111	-0.868	-0.181	-0.181
TS	-0.226	-0.220	-0.220	-0.224	-1.137	-0.763	-0.762
ϵ -greedy	-0.250	-0.229	-0.229	-0.237	-1.00	-0.506	-0.496

directed and random exploration, which leads to more human-like decision behavior. However, in the 4-armed bandit task, these algorithms also fail to engage in effective exploration.

Table 5 reports the average cumulative regret (with standard error) and exploitation rates in the last round across agents for both tasks. The three algorithms show distinct performance patterns: Thompson Sampling (TS) and ϵ -greedy perform poorly in both tasks, while UCB achieves particularly strong results in the 2-armed task but also struggles in the 4-armed task. This reflects the fact that while these algorithms are designed to be asymptotically optimal, yet the 2-armed task has a short time horizon, and the 4-armed task is non-stationary. Notably, TS and ϵ -greedy exhibit the lowest exploitation rate in the 4-armed exploitation rates in the 4-armed task, suggesting that they over-explore in this complex environment.

The remaining tables report full parameter estimates for all choice models fitted to data across all agents from both bandit tasks.

Tables 6 and 7 report the posterior means and standard deviations of the population-level parameters estimated from the SM-3 model in the 4-armed bandit task. Table 6 summarizes the population-level means (μ^x) for each parameter x , while Table 7 reports the corresponding population-level standard deviations (σ^x).

Tables 8 and 9 present the posterior means and standard deviations of the population-level parameters estimated from the SM-2 and SM-1 models, respectively, in the 4-armed bandit task.

Table 2: Exploitation rates in the 2-armed bandit task across different agents

(a) Different LLM versions				(b) Human and algorithmic baselines	
Agent	Basic	CoT	Reasoning	Agent	Exploitation Rate
CHATGPT	0.90	0.92	0.95	Human	0.89
GEMINI	0.92	0.92	0.91	UCB	0.91
DEEPSPEEK	0.91	0.90	0.94	TS	0.88
				ϵ -greedy	0.91

Table 3: Estimated population-level mean parameters for MAB algorithms in the 2-armed bandit task.

Algorithm	β (SM-3)	ϕ (SM-3)	ρ (SM-3)	w_1 (Probit)	w_2 (Probit)	w_3 (Probit)
UCB	0.683 (0.055)	1.402 (0.315)	0.604 (0.240)	0.071 (0.042)	0.408 (0.106)	1.056 (0.166)
TS	0.22 (0.02)	-1.84 (0.62)	0.80 (0.49)	0.06 (0.03)	-0.32 (0.05)	0.18 (0.10)
ϵ -greedy	0.15 (0.01)	-5.63 (1.04)	0.92 (0.67)	0.10 (0.02)	-0.5 (0.05)	-0.10 (0.05)

Table 8 reports the group-level means (μ^x) and standard deviations (σ^x) for each parameter in the SM-2 model, while Table 9 shows the corresponding estimates for the SM-1 model.

Tables 10 and 11 report the posterior means and standard deviations of the population-level parameters estimated from the SM-3 model in the 2-armed bandit task. Table 10 summarizes the population-level means (μ^x) for each parameter, while Table 11 reports the corresponding population-level standard deviations (σ^x).

Tables 12 and 13 present the posterior means and standard deviations of the population-level parameters estimated from the SM-2 and SM-1 models, respectively, in the 2-armed bandit task. Table 12 reports the group-level means (μ^x) and standard deviations (σ^x) for each parameter in the SM-2 model, while Table 13 shows the corresponding estimates for the SM-1 model.

Tables 14 and 15 report the posterior means and standard deviations of the population-level parameters estimated from the Probit model in the 2-armed bandit task. Table 14 summarizes the population-level means (μ^x) for each parameter, while Table 15 reports the corresponding population-level standard deviations (σ^x).

Table 4: Estimated population-level mean parameters for MAB algorithms in the 4-armed bandit task.

Algorithm	β (SM-3)	ϕ (SM-3)	ρ (SM-3)
UCB	0.057 (0.006)	-9.978 (1.149)	-2.486 (1.807)
TS	0.03 (0.01)	-13.17 (0.97)	-4.80 (1.68)
ϵ -greedy	0.13 (0.01)	-0.84 (0.12)	6.02 (0.73)

Table 5: Average cumulative regret and exploitation rates in the last round across both tasks, with standard errors reported for regret.

Agent/Prompt	2-armed bandit task		4-armed bandit task	
	Regret	Exploit Rate	Regret	Exploit Rate
CHATGPT	13.467 (0.911)	0.897	3599.267 (352.296)	0.653
CHATGPT + CoT	12.650 (0.725)	0.921	2472.733 (320.921)	0.698
CHATGPT (R)	14.143 (0.492)	0.952	1803.600 (235.734)	0.821
GEMINI	10.700 (0.763)	0.919	3247.667 (343.501)	0.685
GEMINI + CoT	13.240 (0.626)	0.920	2306.933 (261.677)	0.732
GEMINI (R)	15.653 (0.448)	0.914	1504.400 (169.034)	0.814
DEEPSSEEK	10.943 (0.693)	0.908	3089.467 (314.202)	0.700
DEEPSSEEK + CoT	16.550 (0.556)	0.903	1678.133 (216.983)	0.802
DEEPSSEEK (R)	13.987 (0.464)	0.943	1532.400 (246.638)	0.838
Human	11.281 (0.398)	0.893	1509.355 (125.098)	0.768
UCB	14.723(0.446)	0.908	2307.933(134.985)	0.698
ϵ -Greedy	18.783 (0.829)	0.908	2569.267 (172.651)	0.596
TS	18.377 (0.658)	0.881	3088.000 (195.839)	0.536

Table 6: Posterior means and standard deviations of μ^x estimated from the SM-3 model in the 4-armed bandit task

Agent/Prompt	μ^β	μ^ϕ	μ^ρ
CHATGPT	0.094(0.018)	-7.983(1.606)	6.555(2.819)
CHATGPT + CoT	0.044(0.004)	-10.458(0.995)	2.404(1.763)
CHATGPT(R)	0.103(0.005)	-4.190(0.283)	-3.691(0.835)
GEMINI	0.108(0.009)	-5.419(0.456)	-4.555(1.630)
GEMINI + CoT	0.070(0.004)	-5.782(0.460)	3.000(1.301)
GEMINI (R)	0.096(0.004)	-2.755(0.213)	0.726(0.670)
DEEPSPEEK	0.137(0.016)	-4.419(0.410)	-0.526(1.307)
DEEPSPEEK + CoT	0.092(0.004)	-3.458(0.255)	0.818(0.780)
DEEPSPEEK (R)	0.135(0.006)	-2.460(0.168)	-2.011(0.546)
Human	0.168(0.010)	0.879(0.171)	5.450(0.299)
UCB	0.057(0.006)	-9.978(1.149)	-2.486(1.807)
ϵ - greedy	0.042(0.003)	-7.774(0.630)	15.925(1.896)
TS	0.029(0.002)	-13.179(0.972)	-4.797(1.684)

Table 7: Posterior means and standard deviations of σ^x estimated from the SM-3 model in the 4-armed bandit task

Agent/Prompt	σ^β	σ^ϕ	σ^ρ
CHATGPT	0.023(0.011)	0.165(0.115)	0.184(0.117)
CHATGPT + CoT	0.001(0.001)	0.183(0.113)	0.188(0.097)
CHATGPT(R)	0.004(0.003)	0.120(0.077)	0.189(0.114)
GEMINI	0.005(0.004)	0.183(0.124)	0.197(0.113)
GEMINI + CoT	0.002(0.002)	0.213(0.138)	0.189(0.105)
GEMINI (R)	0.002(0.002)	0.109(0.071)	0.200(0.111)
DEEPSPEEK	0.027(0.016)	0.312(0.197)	0.205(0.118)
DEEPSPEEK + CoT	0.003(0.002)	0.186(0.106)	0.181(0.111)
DEEPSPEEK (R)	0.006(0.004)	0.140(0.090)	0.171(0.114)
Human	0.053(0.008)	0.850(0.085)	0.268(0.162)
UCB	0.006(0.004)	0.182(0.116)	0.188(0.111)
ϵ - greedy	0.001(0.001)	0.177(0.116)	0.217(0.105)
TS	0.003(0.001)	0.149(0.106)	0.172(0.107)

Table 8: Posterior means and standard deviations of μ^x and σ^x estimated from the SM-2 model in the 4-armed bandit task

Agent/Prompt	μ^β	μ^ϕ	σ^β	σ^ϕ
CHATGPT	0.101(0.022)	-8.862(1.660)	0.032(0.016)	0.185(0.115)
CHATGPT + CoT	0.044(0.004)	-10.861(1.081)	0.002(0.001)	0.199(0.110)
CHATGPT(R)	0.098(0.005)	-3.944(0.279)	0.004(0.002)	0.123(0.074)
GEMINI	0.101(0.008)	-5.275(0.422)	0.004(0.004)	0.179(0.109)
GEMINI + CoT	0.072(0.004)	-5.997(0.410)	0.002(0.002)	0.248(0.120)
GEMINI (R)	0.098(0.004)	-2.761(0.197)	0.002(0.002)	0.113(0.072)
DEEPSPEEK	0.138(0.016)	-4.317(0.378)	0.028(0.017)	0.327(0.181)
DEEPSPEEK + CoT	0.092(0.004)	-3.540(0.251)	0.003(0.002)	0.196(0.108)
DEEPSPEEK (R)	0.133(0.007)	-2.261(0.182)	0.006(0.004)	0.121(0.090)
Human	0.168(0.010)	0.159(0.153)	0.051(0.008)	0.767(0.080)
UCB	0.058(0.006)	-9.303(0.973)	0.005(0.004)	0.179(0.110)
ϵ - greedy	0.043(0.003)	-9.975(0.690)	0.001(0.001)	0.212(0.121)
TS	0.030(0.002)	-12.325(0.925)	0.003(0.001)	0.176(0.103)

Table 9: Posterior means and standard deviations of μ^x and σ^x estimated from the SM-1 model in the 4-armed bandit task

Agent/Prompt	μ^β	σ^β
CHATGPT	0.142(0.025)	0.096(0.021)
CHATGPT + CoT	0.150(0.018)	0.067(0.015)
CHATGPT(R)	0.243(0.017)	0.062(0.015)
GEMINI	0.156(0.020)	0.074(0.016)
GEMINI + CoT	0.163(0.015)	0.053(0.012)
GEMINI (R)	0.187(0.005)	0.012(0.006)
DEEPSPEEK	0.205(0.038)	0.140(0.030)
DEEPSPEEK + CoT	0.202(0.013)	0.048(0.012)
DEEPSPEEK (R)	0.257(0.013)	0.044(0.011)
Human	0.161(0.011)	0.058(0.009)
UCB	0.143(0.013)	0.047(0.011)
ϵ - greedy	0.106(0.009)	0.032(0.007)
TS	0.076(0.009)	0.034(0.008)

Table 10: Posterior means and standard deviations of μ^x estimated from the SM-3 model in the 2-armed bandit task

Agent/Prompt	μ^β	μ^ϕ	μ^ρ
CHATGPT	0.206(0.010)	-0.264(0.093)	0.591(0.402)
CHATGPT + CoT	0.291(0.015)	0.108(0.071)	-0.099(0.332)
CHATGPT(R)	0.416(0.025)	2.562(0.092)	4.638(0.366)
GEMINI	0.317(0.016)	-0.563(0.068)	-2.228(0.309)
GEMINI + CoT	0.267(0.015)	0.140(0.089)	-0.418(0.317)
GEMINI (R)	0.297(0.015)	1.669(0.109)	1.936(0.325)
DEEPSEEK	0.265(0.016)	-0.220(0.077)	0.520(0.351)
DEEPSEEK + CoT	0.319(0.022)	2.552(0.174)	2.021(0.322)
DEEPSEEK (R)	0.590(0.059)	3.613(0.124)	4.719(0.300)
Human	0.436(0.024)	1.075(0.138)	1.076(0.273)
UCB	0.683(0.055)	1.402(0.315)	0.604(0.240)
ϵ - greedy	0.152(0.013)	-5.631(1.048)	0.928(0.673)
TS	0.224(0.017)	-1.842(0.625)	0.796(0.492)

Table 11: Posterior means and standard deviations of σ^x estimated from the SM-3 model in the 2-armed bandit task

Agent/Prompt	σ^β	σ^ϕ	σ^ρ
CHATGPT	0.011(0.009)	0.081(0.060)	0.328(0.215)
CHATGPT + CoT	0.024(0.014)	0.090(0.058)	0.330(0.218)
CHATGPT(R)	0.025(0.018)	0.120(0.075)	0.369(0.262)
GEMINI	0.018(0.012)	0.055(0.039)	0.300(0.215)
GEMINI + CoT	0.022(0.015)	0.196(0.087)	0.351(0.235)
GEMINI (R)	0.017(0.012)	0.257(0.104)	0.382(0.249)
DEEPSEEK	0.022(0.012)	0.056(0.046)	0.347(0.290)
DEEPSEEK + CoT	0.053(0.024)	0.498(0.149)	0.334(0.226)
DEEPSEEK (R)	0.154(0.065)	0.120(0.080)	0.340(0.218)
Human	0.135(0.022)	0.849(0.103)	1.546(0.224)
UCB	0.057(0.047)	0.307(0.206)	0.267(0.178)
ϵ - greedy	0.019(0.010)	0.922(0.578)	0.550(0.421)
TS	0.032(0.015)	0.433(0.289)	0.426(0.283)

Table 12: Posterior means and standard deviations of μ^x and σ^x estimated from the SM-2 model in the 2-armed bandit task

Agent/Prompt	μ^β	μ^ϕ	σ^β	σ^ϕ
CHATGPT	0.208(0.012)	-0.329(0.072)	0.012(0.009)	0.071(0.057)
CHATGPT + CoT	0.291(0.014)	0.125(0.059)	0.023(0.014)	0.090(0.062)
CHATGPT(R)	0.469(0.024)	1.555(0.062)	0.028(0.019)	0.093(0.066)
GEMINI	0.280(0.014)	-0.321(0.062)	0.017(0.012)	0.061(0.039)
GEMINI + CoT	0.261(0.013)	0.184(0.081)	0.022(0.014)	0.192(0.086)
GEMINI (R)	0.324(0.015)	1.344(0.089)	0.019(0.013)	0.227(0.100)
DEEPSEEK	0.274(0.014)	-0.266(0.065)	0.024(0.016)	0.065(0.046)
DEEPSEEK + CoT	0.347(0.025)	2.098(0.126)	0.067(0.028)	0.361(0.122)
DEEPSEEK (R)	0.532(0.034)	2.006(0.072)	0.063(0.038)	0.103(0.068)
Human	0.463(0.027)	0.873(0.129)	0.151(0.024)	0.828(0.104)
UCB	0.674(0.056)	0.888(0.254)	0.075(0.050)	0.333(0.207)
ϵ - greedy	0.152(0.013)	-6.305(0.982)	0.020(0.010)	0.850(0.592)
TS	0.222(0.017)	-2.448(0.518)	0.032(0.015)	0.421(0.295)

Table 13: Posterior means and standard deviations of μ^x and σ^x estimated from the SM-1 model in the 2-armed bandit task

Agent/Prompt	μ^β	σ^β
CHATGPT	0.232(0.010)	0.016(0.011)
CHATGPT + CoT	0.277(0.011)	0.018(0.012)
CHATGPT(R)	0.247(0.010)	0.011(0.008)
GEMINI	0.312(0.014)	0.021(0.014)
GEMINI + CoT	0.245(0.012)	0.023(0.013)
GEMINI (R)	0.207(0.008)	0.009(0.007)
DEEPSEEK	0.300(0.015)	0.031(0.016)
DEEPSEEK + CoT	0.190(0.008)	0.010(0.008)
DEEPSEEK (R)	0.241(0.010)	0.012(0.008)
Human	0.313(0.014)	0.080(0.013)
UCB	0.556(0.032)	0.038(0.027)
ϵ - greedy	0.260(0.024)	0.072(0.026)
TS	0.286(0.021)	0.061(0.022)

Table 14: Posterior means and standard deviations of μ^x estimated from the probit model in the 2-armed bandit task

Agent/Prompt	μ^{w_1}	μ^{w_2}	μ^{w_3}
CHATGPT	0.162(0.012)	-0.028(0.010)	-0.181(0.040)
CHATGPT + CoT	0.195(0.014)	0.033(0.012)	-0.169(0.048)
CHATGPT(R)	0.003(0.002)	0.383(0.024)	1.860(0.092)
GEMINI	0.288(0.020)	-0.041(0.011)	-0.481(0.061)
GEMINI + CoT	0.108(0.012)	0.010(0.013)	0.108(0.046)
GEMINI (R)	0.016(0.013)	0.146(0.021)	0.720(0.050)
DEEPSEEK	0.355(0.027)	-0.007(0.014)	-0.711(0.078)
DEEPSEEK + CoT	0.001(0.015)	0.205(0.023)	0.638(0.057)
DEEPSEEK (R)	0.006(0.004)	0.660(0.066)	1.952(0.217)
Human	0.025(0.021)	0.140(0.023)	0.877(0.091)
UCB	0.071(0.042)	0.408(0.106)	1.056(0.166)
ϵ - greedy	0.101(0.018)	-0.563(0.051)	-0.096(0.057)
TS	0.064(0.029)	-0.321(0.053)	0.178(0.099)

Table 15: Posterior means and standard deviations of σ^x estimated from the probit model in the 2-armed bandit task

Agent/Prompt	σ^{w_1}	σ^{w_2}	σ^{w_3}
CHATGPT	0.010(0.006)	0.011(0.008)	0.028(0.019)
CHATGPT + CoT	0.013(0.008)	0.018(0.012)	0.037(0.025)
CHATGPT(R)	0.001(0.001)	0.021(0.014)	0.067(0.050)
GEMINI	0.010(0.007)	0.011(0.009)	0.029(0.019)
GEMINI + CoT	0.014(0.012)	0.028(0.015)	0.060(0.047)
GEMINI (R)	0.012(0.007)	0.019(0.015)	0.070(0.044)
DEEPSEEK	0.019(0.012)	0.020(0.014)	0.033(0.028)
DEEPSEEK + CoT	0.030(0.012)	0.057(0.024)	0.102(0.049)
DEEPSEEK (R)	0.002(0.002)	0.166(0.066)	0.671(0.164)
Human	0.113(0.019)	0.139(0.020)	0.498(0.080)
UCB	0.019(0.015)	0.133(0.087)	0.133(0.081)
ϵ - greedy	0.012(0.007)	0.096(0.056)	0.028(0.026)
TS	0.022(0.012)	0.057(0.040)	0.069(0.039)

D Future Work and Limitations

While our work reveals systematic differences between LLMs and human E&E strategies in MAB tasks, we do not directly address how to reduce these discrepancies. In particular, we do not propose specific methods to align LLM behavior more closely with human strategies. Future work could explore techniques such as prompt engineering, instruction fine-tuning, or reinforcement learning to guide LLMs toward more adaptive, human-like exploration policies.

Another key limitation of our current study is that our human dataset does not include demographic features (e.g., age, sex, education level, race), which could influence decision-making strategies. Consequently, our LLM evaluation does not account for such individual-level variability, and we do not incorporate such demographic attributes into LLM prompts. Future work could explore how incorporating such information impacts LLMs' behavior and their alignment with human strategies.